The Astrophysical Journal, 588:1072–1081, 2003 May 10

OXYGEN ABUNDANCE IN THE TEMPLATE HALO GIANT HD 122563[1]

Beatriz Barbuy
Universidade de São Paulo, IAG, CP 3386, São Paulo 01060-970, Brazil; barbuy@astro.iag.usp.br

Jorge Meléndez
Universidad Nacional Mayor de San Marcos, Facultad de Ciencias Fisicas, Avenada Venezuela S/N, Ciudad Universitaria, Lima, Peru; jorge@astro.iag.usp.br

Monique Spite, François Spite, Eric Depagne, and Vanessa Hill
Observatoire de Paris-Meudon, GEPI, 92195 Meudon Cedex, France; Monique.Spite@obspm.fr, Francois.Spite@obspm.fr, Eric.Depagne@obspm.fr, Vanessa.Hill@obspm.fr

Roger Cayrel
Observatoire de Paris, GEPI, 61 avenue de l'Observatoire, 75014 Paris, France; Roger.Cayrel@obspm.fr

Piercarlo Bonifacio
INAF, Osservatorio Astronomico di Trieste, via G.B. Tiepolo 11, 34131 Trieste, Italy; bonifaci@ts.astro.it

Augusto Damineli
Universidade de São Paulo, IAG, CP 3386, São Paulo 01060-970, Brazil; damineli@astro.iag.usp.br

and

Carlos A. O. Torres
Laboratório Nacional de Astrofísica/MCT, Itajubá, Brazil; and European Southern Observatory, Casilla 19, Santiago, Chile; beto@lna.br, ctorres@eso.org

Received 2002 October 23; accepted 2003 January 21

ABSTRACT

HD 122563 is a well-known bright ($V = 6.2$) halo giant of low metallicity ([Fe/H] ≈ -2.7). We have observed HD 122563 for infrared OH lines at 1.5–1.7 μm in the H band with the NIRSPEC high-resolution spectrograph at the 10 m Keck Telescope. Optical spectra were obtained with the UVES spectrograph at the 8 m VLT UT2 telescope at ESO (Paranal) and the FEROS spectrograph at ESO (La Silla). Based on the optical high-resolution data, a detailed analysis has been carried out, and data on the forbidden [O I] 6300 Å line, unblended by telluric or sky lines, was obtained with the FEROS spectrograph. Signal-to-noise ratios of 200–400 were obtained at resolutions of 37,000 in the H band and 45,000 in the optical. For the analysis we have adopted a photometric effective temperature $T_{\rm eff} = 4600$ K. Two values for the gravity were adopted: a value deduced from ionization equilibrium, $\log g = 1.1$, with corresponding metallicity [Fe/H] $= -2.8$ and microturbulence velocity $v_t = 2.0$ km s^{-1}; and $\log g = 1.5$, derived from the *Hipparcos* parallax, implying [Fe/H] $= -2.71$ and $v_t = 2.0$ km s^{-1}. The forbidden [O I] 6300 Å and the permitted O I 7771 Å lines give O/Fe ratios essentially insensitive to model parameter variations, whereas the oxygen abundances from OH lines are sensitive to gravity, giving [O/Fe] $= +0.9$ and $+0.7$, respectively, for $\log g = 1.1$ and 1.5. We derive the following oxygen abundances: for model 1, [O/Fe] $= +0.6$, $+1.1$, and $+0.9$; and for model 2, [O/Fe] $= +0.6$, $+1.1$, and $+0.7$, based on the [O I] 6300 Å, O I 7771 Å, and IR OH 1.6 μm lines, respectively. The different oxygen abundance indicators give different oxygen abundances, illustrating the problem of oxygen abundance derivation in metal-poor giants. This is important because the age of globular clusters and the production of Li, Be, and B from spallation of C, N, and O atoms in the early Galaxy depend on the oxygen abundance adopted for the metal-poor stars.

Subject headings: stars: abundances — stars: individual (HD 122563) — stars: Population II

On-line material: machine-readable table

1. INTRODUCTION

Further progress in theories of the nucleosynthesis and chemical evolution of galaxies requires progressively more accurate determinations of element abundances in stars of various ages and metallicities. In particular, metal-poor stars are landmarks of the metal enrichment of galaxies, and they are more difficult to analyze than stars similar to the Sun. Solar-like stars, for example, benefit from our detailed knowledge of the solar atmosphere model. The lower opacity of the atmospheres of metal-poor stars, however, creates difficulties in the analyses which, although discussed in the literature, have not yet reached generally accepted solutions.

HD 122563 has been among the best studied halo giants since its discovery by Wallerstein et al. (1963). It has low metallicity ([Fe/H] ~ -2.7), a bright magnitude of $V = 6.20$, a null reddening $E(B-V) = 0$, and is observable from both hemispheres. Accurate photometric measurements are available in several color systems (numerous and accurate enough to suggest a slight variability). The small

[1] Observations carried out with the Keck Telescope, Mauna Kea, Hawaii, within the Gemini-Keck agreement, the Very Large Telescope at the European Southern Observatory (ESO), Paranal, Chile, and the 1.5 m ESO telescope at ESO, La Silla, Chile.

distance of the star allowed the *Hipparcos* satellite to measure its parallax. This provides a useful constraint on the absolute luminosity (surface gravity) of the star.

Several detailed analyses are found in the literature, most of them in rough agreement concerning the derived atmospheric parameters. Effective temperatures are in the range $4400 < T_{\rm eff} < 4700$ K, while $0.5 < \log g < 1.5$, and $-2.9 < [{\rm Fe/H}] < -2.5$. These ranges seem rather large, considering the reported quality of the observational data, and may be an indication of the inadequacy of the model atmospheres as an accurate representation of the complex real atmosphere of the star.

Oxygen abundances in metal-poor stars have been a controversial issue in the last few years. Israelian et al. (1998, 2001) and Boesgaard et al. (1999) have claimed that the [O/Fe] ratio in metal-poor stars increases more or less linearly toward lower metallicities, based on lines of the UV OH $A^2\Sigma^+$–$X^2\Pi$ system. On the other hand, Carretta, Gratton, & Sneden (2000), based on [O I] 6300 Å and the permitted O I 7771–7775 Å triplet, find that their data support the presence of a plateau in the O/Fe ratios of metal-poor stars. The recent data of Nissen et al. (2002), when standard one-dimensional model atmospheres are used for unevolved metal-poor stars, support a double-slope linear rise of [O/Fe], with $d[{\rm O/Fe}]/d[{\rm Fe/H}] \approx 0.4$ in the interval $0.0 < [{\rm Fe/H}] < -0.75$, and $d[{\rm O/Fe}]/d[{\rm Fe/H}] \approx 0.2$ in the interval $-0.75 < [{\rm Fe/H}] < -2.5$. If three-dimensional model atmospheres that take into account the effects of granulation are used instead, the slope in the $-0.75 < [{\rm Fe/H}] < -2.5$ segment becomes much smaller, almost a plateau. However, it should be noted that the three-dimensional computations of Nissen et al. (2002) were done in LTE. Kiselman (1998) and Cayrel & Steffen (2000) have shown that NLTE makes a significant change, at least in the case of the Li I ion. Therefore, the three-dimensional results presented by Nissen et al. (2002), or similar ones based on LTE transfer in three-dimensional model atmospheres, should be viewed with caution until confirmed by full NLTE computations.

Awaiting such computations for both lines and continua using three-dimensional model atmospheres, it is of crucial importance to determine the oxygen abundance in the bright and well-studied star HD 122563 using classical model atmospheres. This star can in fact be considered representative of the halo giants, and it allows us to highlight the systematic effects on oxygen abundance determinations based on different lines. This will provide a cornerstone for the oxygen abundances found in the literature from classical models for numerous halo giants.

In the present work we use the infrared first-overtone (IR) $X^2\Pi$ vibration-rotation transitions of OH lines in the region 1.5–1.7 μm to derive the oxygen abundance of HD 122563. We also derive the oxygen abundance from the forbidden [O I] 6300.31 Å line and the permitted O I 7771 Å line. In the visible domain, the lines of various other elements are measured, providing abundances in the LTE approximation, but also providing various dependences of the abundances on the atmospheric parameters. Classical one-dimensional model atmospheres are used throughout the paper.

We present the observations in § 2, and describe the detailed analysis in § 3. The results on oxygen abundances are discussed in § 4. The abundances of other elements are briefly described in § 5, and in § 6 we offer our conclusions.

2. OBSERVATIONS

2.1. *Data Acquisition and Reduction*

Table 1 presents the journal of observations. High-resolution infrared spectra were obtained from images taken at the 10 m Keck telescope, using the NIRSPEC spectrograph (McLean et al. 1998). FWHM resolutions of 37,000 were achieved with the échelle grating, with a 2 pixel projected slit width. The detector is an Aladdin 1024×1024 InSb array, covering essentially all the H band in the range 1.5–1.7 μm, apart from small gaps (0.008 μm) between the orders. More details are given in Meléndez & Barbuy (2002, hereafter MB02). A signal-to-noise ratio S/N $\approx$ 250 in the IR was estimated from continuum regions.

For the VLT-UVES observations, the spectrograph setup (dichroic mode, central wavelength at 396 nm in the blue arm and 573 and 850 nm in the red arm) provided a spectral coverage from 330 to 1041 nm, with a gap between 458 and 471 nm, around the dichroic splitting wavelength, and two small gaps around 573 and 850 nm, due to the gap between the two CCDs of the mosaic in the red arm. The entrance slit of 1″ yielded a resolving power of 43,000. The spectra were reduced using the ECHELLE reduction package within MIDAS. The S/N of a single 75 s spectrum was $\approx$370 around 615 nm and 300 at 777 nm. A heliocentric radial velocity of $v_r = -26.4$ km s^{-1} was measured from the UVES spectra.

Spectra in the visible domain were also obtained at the 1.52 m telescope at ESO, La Silla, using the Fiber-fed Extended-Range Optical Spectrograph (FEROS) (Kaufer et al. 2000). The useful spectrum coverage is from 380 to 880

TABLE 1

Log of Observations of HD 122563, $V = 6.20$

Date	Exposure (s)	S/N	Wavelength	Telescope
2000 May 20.....	4×120	250	1.46–1.70 μm	10 m Keck
2002 Mar 18	600	180	360–900 nm	1.52 m ESO
2002 Mar 18	600	255	360–900 nm	1.52 m ESO
2002 Apr 01.....	600	260	360–900 nm	1.52 m ESO
2000 Jul 18	75	370 (615 nm)	471–675 nm	8 m VLT Kueyen ESO
2000 Jul 18	75	390 (615 nm)	471–675 nm	8 m VLT Kueyen ESO
2000 Jul 18	75	305 (777 nm)	659–1041 nm	8 m VLT Kueyen ESO
2000 Jul 18	75	267 (777 nm)	659–1041 nm	8 m VLT Kueyen ESO

TABLE 2
HD 122563 Colors

Color	Value
$(b-y)_0$	0.638
$(V-R)_0^{\rm J}$	0.805
$(J-K)_0^{\rm TCS}$	0.606
$(V-K)_0^{\rm TCS}$	2.502

Note.—J = Johnson, TCS = Telescopio Carlos Sánchez.

nm, with a resolving power of 48,000. Two fibers, with entrance aperture of 2.″7, simultaneously recorded star light and sky background. The detector is a back-illuminated CCD with 2948 × 4096 pixels of 15 μm size.

HD 122563 was observed on 2002 March 18 and April 1; these dates were suitable for avoiding any blending of the oxygen forbidden [O I] 6300 Å line by nearby telluric lines or the sky emission line (see § 3.6.2). Using a special package for reductions (DRS) of FEROS data, in the MIDAS environment, the data reduction proceeded with subtraction of bias and scattered light in the CCD, orders extraction, flat-fielding, and wavelength calibration. S/N ≈ 200 around 600 nm were obtained. A heliocentric radial velocity of $v_r = -26.5 \pm 0.2$ km s^{-1} was measured from the FEROS spectrum of April 1.

3. DETAILED ANALYSIS

3.1. *Effective Temperatures*

Colors available in the literature for HD 122563, given in Table 2, were taken from the following sources: *J*, *H*, and *K* in the Telescopio Carlos Sánchez (TCS) system from Alonso, Arribas, & Martínez-Roger (1998); Strömgren *ubvy*-β from the Catalogue by Hauck & Mermilliod (1998); and $V-R$ from Stone (1983). The distance was determined from the *Hipparcos* parallax (Perryman et al. 1997), and a reddening value $E(B-V) = 0$ was estimated by using the models of reddening maps by Hakkila et al. (1997) and Chen et al. (1998).

Effective temperatures $T_{\rm eff}$ derived using the $b-y$, $V-R$, $V-K$, and $J-K$ calibrations of Alonso, Arribas, & Martínez-Roger (1999a, hereafter AAM99a) are given in Table 3. This table also shows an infrared flux method (IRFM AAM99b) temperature, as determined by Alonso, Arribas, & Martínez-Roger (1999b, hereafter AAM99b). The mean of the IRFM calibrations (AAM99a), which is essentially the same as the IRFM determination by AAM99b, is shown in the bottom row of Table 3.

TABLE 3
HD 122563 Effective Temperatures Based on Different Methods (§ 3.1)

Method	$T_{\rm eff}$ (K)
IRFM calibration (AAM99a):	
$b-y$	4626
$V-R$	4595
$V-K$	4583/4559
$J-K$	4657
mean	4615
IRFM AAM99b	4572
IRFM mean	4594

TABLE 4
Line List

λ (Å)	Ion	$\chi_{\rm ex}$ (eV)	log gf	EW$_{\rm UVES}$ (mÅ)	EW$_{\rm FEROS}$ (mÅ)
3805.349.....	Fe I	3.30	+0.31	62.3	66
3815.851.....	Fe I	1.48	+0.24	169.0	
3820.436.....	Fe I	0.86	+0.12	264.5	
3825.891.....	Fe I	0.91	−0.04	218.3	
3827.832.....	Fe I	1.56	+0.06	161.5	168
3840.447.....	Fe I	0.99	−0.51	174.5	169
3849.977.....	Fe I	1.01	−0.87	140.0	149
3850.826.....	Fe I	0.99	−1.73	122.0	
3856.381.....	Fe I	0.05	−1.29	179.1	
3859.922.....	Fe I	0.00	−0.71	234.9	

Note.—Table 4 is published in its entirety in the electronic edition of the *Astrophysical Journal*. A portion is shown here for guidance regarding its form and content.

3.2. *Equivalent Widths, Oscillator Strengths, and Damping Constants*

Equivalent widths of Fe I and Fe II were measured on the optical high-resolution spectra obtained with the VLT-UVES and FEROS spectrographs at ESO.

Table 4 lists the equivalent widths measured from the VLT and FEROS spectra for Fe I and Fe II lines; a comparison between those values gives $\delta({\rm EW}) = {\rm EW_{FEROS}} - {\rm EW_{UVES}} = 1.2 \pm 0.04$ mÅ ($\sigma = 0.3$ mÅ). We also compared the equivalent widths measured from the FEROS spectra with those from McDonald Observatory (Westin et al. 2000). We have 175 lines in common with the coudé/McDonald spectrograph, resulting in $\delta({\rm EW}) = {\rm EW_{FEROS}} - {\rm EW_{McDonald}} = -0.6 \pm 0.2$ mÅ ($\sigma = 2.4$ mÅ). A comparison with data from Johnson (2002), obtained with the HIRES spectrograph at Keck and the Hamilton spectrograph at the Lick 3 m telescope, gives $\delta({\rm EW}) = {\rm EW_{HIRES/Hamilton}} - {\rm EW_{UVES}} = 2.75 \pm 0.2$ mÅ ($\sigma = 3.6$ mÅ).

Oscillator strengths for Fe I lines were adopted from the NIST database; these are very close to those of O'Brian et al. (1991), the latter being about 0.02 higher on average. For Fe II lines we have adopted theoretical *gf* values of Biémont et al. (1991), and data from the VALD-2 compilation by Kupka et al. (2000).[2] Ti I and Ti II data are also from VALD-2.

The damping constants were computed based on the tables of damping constants from the collisional broadening theory of Anstee, O'Mara, & Ross (1997), Anstee & O'Mara (1995), Barklem & O'Mara (1997), and Barklem, O'Mara, & Ross (1998).

3.3. *Calculations*

For our calculations, we used OSMARCS model atmospheres. These one-dimensional models were originally developed by Bell et al. (1976) and Gustafsson et al. (1975), and they were further improved by Plez, Brett, & Nordlund (1992), Edvardsson et al. (1993), and Asplund et al. (1997).

[2] Available at http://www.astro.univie.ac.at/~vald.

TABLE 5
ATMOSPHERIC PARAMETERS OF HD 122563 FROM MODELS 1 AND 2

Model	$T_{\rm eff}$ (K)	$\log g$	[Fe/H]	v_t (km s^{-1})	[C/Fe]	[O I 6300/Fe]	[O I 7771/Fe]	[OH/Fe]
1.....	4600	1.1	−2.80	2.0	−0.40	+0.6	+1.1	0.84–1.05 (0.90)
2.....	4600	1.5	−2.71	2.0	−0.60	+0.6	+1.1	0.60–0.82 (0.70)

NOTE.—Model 1 obtained from a spectroscopic determination; model 2 from photometric temperature, trigonometric gravity, and [Fe/H].

We used the LTE spectrum synthesis codes described in Plez, Smith, & Lambert (1993) and Alvarez & Plez (1998), as well as that of Cayrel et al. (1991).

3.4. *Gravity*

The *Hipparcos* parallax, $\pi = 3.76 \pm 0.72$ mas, is used to derive a trigonometric gravity, using the classical relations (see, e.g., Nissen, Høg, & Schuster 1997)

$$\frac{\log g}{g_\odot} = \frac{\log M}{M_\odot} + \frac{4 \log T_{\rm eff}}{T_{\rm eff}} + 0.4(M_{\rm bol} - M_{\rm bol,\odot}) \ ,$$

with

$$M_{\rm bol} = V_0 + {\rm BC} + 5 \log \pi + 5 \ ,$$

where BC is the bolometric correction, the parallax π is given in arcseconds, and the solar bolometric magnitude $M_{\rm bol,\odot} = 4.75$; we adopt a mass of 0.8 $M_\odot$ for HD 122563. The $m_{\rm bol}$ ($= V_0 + {\rm BC}$) for HD 122563 is derived directly from its bolometric flux measured by AAM99b of $F_{\rm bol} = 1.248 \times 10^{-7}$, and using $m_{\rm bol} = -2.5 \log F_{\rm bol}({\rm cgs}) - 11.4822$, this gives $m_{\rm bol}({\rm HD\ 122563}) = 5.78$.

The resulting gravity value for $T_{\rm eff} = 4600$ K is $\log g = 1.53$. Therefore, a trigonometric $\log g = 1.5$ is adopted. A gravity value derived from such a small parallax is uncertain; the $\pm 1\ \sigma$ range is $1.3 < \log g < 1.7$. On the other hand, a spectroscopic determination of gravity using the ionization equilibrium between Fe I and Fe II combined with that of Ti I and Ti II (see § 3.5) gives a best value of $\log g = 1.1$. However, it is to be noted that there are NLTE effects on the Fe I lines. Such effects were computed by Dalle Ore (1993), in particular for HD 122563.

3.5. *Metallicity and Microturbulence Velocity*

We derive the stellar parameters for HD 122563 in two ways, summarized in Table 5:

Model 1.—Adopts the photometric effective temperature of $T_{\rm eff} = 4600$ K, and requires ionization equilibrium, deriving $\log g = 1.1$, and abundances of Fe I and Fe II of [Fe I/H] = −2.77 and [Fe II/H] = −2.84, as indicated in the top half of Table 6, where [Fe/H] = −2.8 is adopted, together with $v_t = 2.0$ km s^{-1}.

Model 2.—Adopts the photometric effective temperature of $T_{\rm eff} = 4600$ K and the gravity of $\log g = 1.5$ derived from the *Hipparcos* parallax, using our equivalent widths to derive metallicity and microturbulent velocity values of [Fe I/H] = −2.86 and [Fe II/H] = −2.71, where [Fe/H] = −2.71 is adopted, together with $v_t = 2.0$ km s^{-1}. The derived abundances are indicated in the bottom half of Table 6.

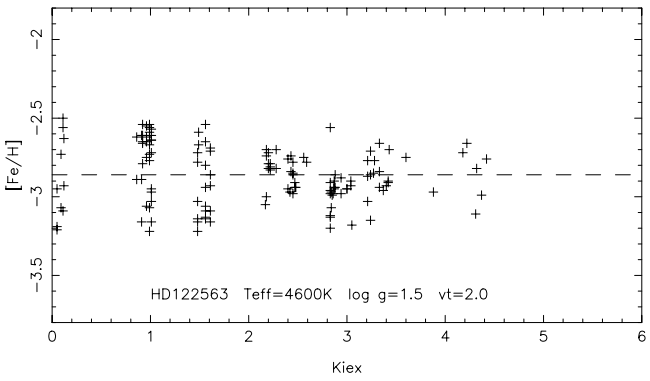

FIG. 1.—Metallicity derived as a function of excitation potential, $\chi_{\rm ex}$

The [Fe/H] obtained as a function of excitation potential and equivalent widths are shown in Figures 1 and 2 for the parameters of model 2.

It is important to note that, relative to MB02, the metallicities derived here are about 0.05 dex lower, as a result of a different set of lines and corresponding oscillator strengths. A main difference in the two calculations is the use of Ti I and Ti II lines to impose ionization equilibrium, together with Fe I and Fe II; in addition to that, in MB02 the *gf*-values of Fe II lines were somewhat different from the present ones, given that they were calibrated with experimental data by taking lifetimes of upper levels and branching ratios and recomputing the *gf*-values; these values were gathered in multiplets, and corrections were applied from comparisons between the theoretical and laboratory values (see more details in MB02). The calculations carried out for the derivation of basic stellar parameters of HD 122563 in the present work are consistent with those in Depagne et al. (2002).

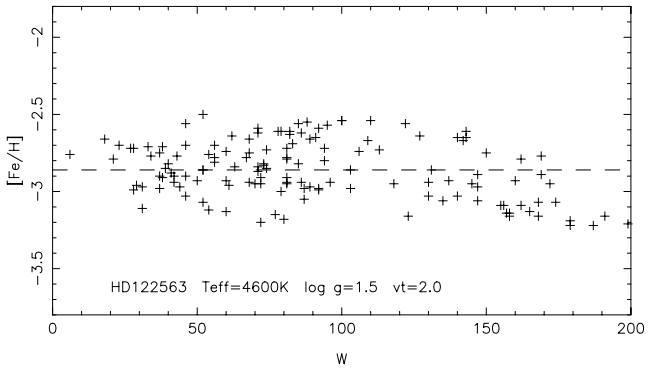

FIG. 2.—Metallicity derived as a function of equivalent width

TABLE 6
ABUNDANCES DERIVED FOR MODELS 1 AND 2

Species	Solar Abundance	Stellar Abundance	[X/H]	[X/Fe]	σ	No. Lines	No. Lines Used
			Model 1				
Na I	6.33	3.77	−2.56	...	0.24	2	2
Mg I	7.58	5.23	−2.35	+0.45	0.14	5	5
Al I	6.47	3.28	−3.18	−0.38	0.08	2	2
Si I	7.55	5.27	−2.28	+0.52	0.00	1	1
K I	5.12	2.82	−2.30	+0.50	0.00	1	1
Ca I	6.36	3.86	−2.50	+0.30	0.10	17	16
Sc II	3.17	0.47	−2.70	+0.10	0.10	7	7
Ti I	5.02	2.33	−2.69	+0.11	0.10	14	14
Ti II	5.02	2.38	−2.64	+0.16	0.12	29	29
Cr I	5.67	2.47	−3.20	...	0.17	7	7
Mn I	5.39	2.45	−2.94	...	0.16	5	5
Fe I	7.50	4.73	−2.77	...	0.18	144	142
Fe II	7.50	4.66	−2.84	...	0.13	18	18
Co I	4.92	2.40	−2.52	...	0.14	4	4
Ni I	6.25	3.58	−2.67	...	0.18	4	4
Zn I	4.60	1.97	−2.63	...	0.00	1	1
			Model 2				
Na I	6.33	3.65	−2.68	+0.03	0.17	2	2
Mg I	7.58	5.14	−2.44	+0.27	0.15	5	5
Al I	6.47	3.14	−3.33	−0.62	0.09	2	2
Si I	7.55	5.22	−2.33	+0.38	0.00	1	1
K I	5.12	2.79	−2.33	+0.38	0.00	1	1
Ca I	6.36	3.82	−2.54	+0.17	0.09	17	16
Sc II	3.17	0.57	−2.60	+0.11	0.10	7	7
Ti I	5.02	2.28	−2.74	−0.03	0.10	14	14
Ti II	5.02	2.50	−2.52	+0.19	0.09	29	26
Cr I	5.67	2.40	−3.27	...	0.19	7	7
Mn I	5.39	2.35	−3.04	...	0.10	5	5
Fe I	7.50	4.64	−2.86	...	0.20	144	143
Fe II	7.50	4.79	−2.71	...	0.14	18	18
Co I	4.92	2.32	−2.60	...	0.14	4	4
Ni I	6.25	3.50	−2.75	...	0.23	4	4
Zn I	4.60	2.03	−2.57	...	0.00	1	1

Model 1: $T_{\rm eff} = 4600$ K, $\log g = 1.1$, [Fe/H] = −2.8, $v_t = 2.0$ km s^{-1}. Model 2: $T_{\rm eff} = 4600$ K, $\log g = 1.5$, [Fe/H] = −2.71, $v_t = 2.0$ km s^{-1}. The overabundances relative to Fe are indicated for the light and α-elements.

We also checked the Johnson (2002) parameters, adopting their $T_{\rm eff} = 4450$ K and $\log g = 0.5$, and using our equivalent widths with the code of Alvarez & Plez (1998), deriving [Fe I/H] = −2.85 and [Fe II/H] = −2.99, together with $v_t = 1.8$ km s^{-1}.

3.6. *Oxygen Abundance*

The oxygen abundances were derived from fits of synthetic spectra to the sample spectra. The LTE code for spectrum synthesis described in Cayrel et al. (1991) was used for the calculations of the OH and CH bands, and also that of Alvarez & Plez (1998) for CH.

The oxygen abundance derived depends on the carbon abundance adopted because a significant fraction of O is locked into CO molecules. The carbon abundance was derived from the CH $A^2\Pi$–$X^2\Sigma$ G band at ∼4300 Å. Details of the atomic and molecular database used are described in Castilho et al. (1999); the code of Alvarez & Plez (1998) uses the CH data described in Hill et al. (2002). The observed and synthetic spectra of the G band of HD 122563, computed with the Hill et al. data, are shown in Figure 3. Our result of [C/Fe] = −0.4 to −0.6 is compatible with the results given by Kraft et al. (1982) of [C/Fe] = −0.5, and by Westin et al. (2000) of [C/Fe] = −0.46. The nitrogen abundance of [N/Fe] = +1.2 was adopted from Sneden (1973), noting that the N abundance has essentially no effect on the derivation of the oxygen abundance. We now describe the

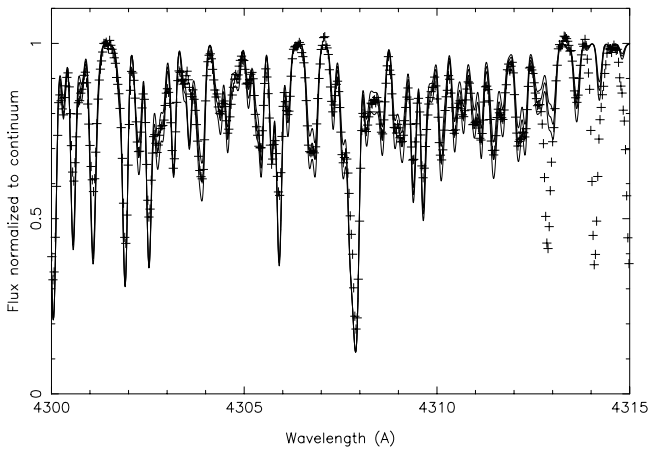

FIG. 3.—G band in HD 122563: observed spectrum (*crosses*) compared to synthetic spectra computed with [C/Fe] = −0.5, −0.6, and −0.7 (*solid lines*) for model 2. The value [C/Fe] = −0.6 is adopted.

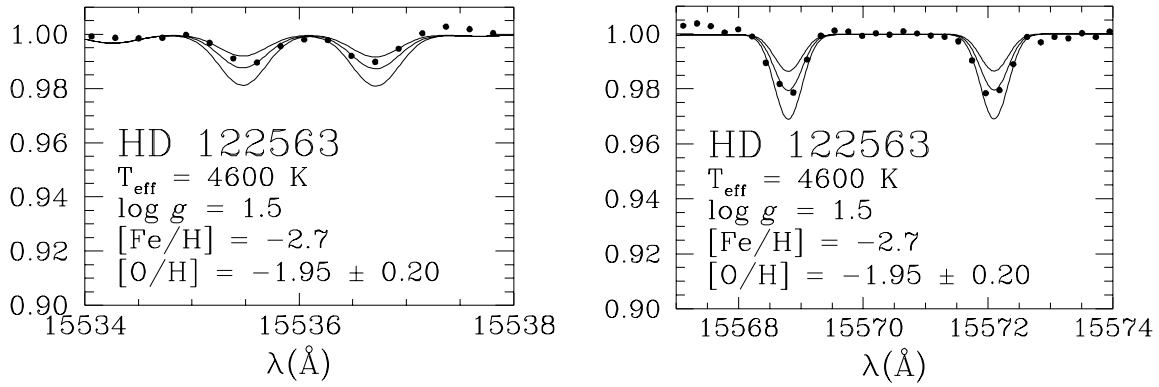

FIG. 4.—IR OH lines in HD 122563: observed spectrum (*filled circles*) compared to synthetic spectra computed with [O/H] = −2.15, −1.95, and −1.75 (*solid lines*), adopting model 2 of Table 5. The value [O/H] = −1.9 or [O/Fe] = +0.7 is adopted.

derivation of oxygen abundance for HD 122563 based on the different lines.

3.6.1. OH *Bands*

The calculations of OH lines in the *H* band were carried out taking into account the atomic line lists described by Meléndez & Barbuy (1999) and Meléndez (1999), together with molecular lines of CN $A^2\Pi$–$X^2\Sigma$, CO $X^1\Sigma^+$ (Meléndez & Barbuy 1999), and OH ($X^2\Pi$) (Meléndez, Barbuy, & Spite 2001). The spectra of selected OH lines of HD 122563, compared to the calculations of model 2, are shown in Figure 4.

The infrared OH vibration-rotation lines ($X^2\Pi$) used in this work are from the first-overtone ($\Delta v = 2$) sequence. Laboratory line lists from the work of Abrams et al. (1994), with wavenumbers and identifications, were kindly provided by S. P. Davis. Energy levels for the OH lines were computed from molecular parameters given in Coxon & Foster (1992) and Abrams et al. (1994). Molecular oscillator strengths were calculated from Einstein coefficients given by Goldman et al. (1998). A dissociation potential $D_0(\mathrm{OH}) = 4.392$ eV (Huber & Herzberg 1979) was adopted.

The list of OH lines used for oxygen abundance determination, together with their molecular *gf*-values, energy levels, and equivalent widths, are given in Table 7. As noted in MB02, the oxygen abundances derived increase with the equivalent width of the OH line. We assume that the weaker lines give the more reliable results, so that an oxygen abundance [O/Fe] = +0.9 is obtained from a mean of the weaker lines given in Table 7 for model 1, whereas [O/Fe] = +0.7 is obtained for model 2.

3.6.2. *The* [O I] 6300 Å *Forbidden Line*

The observation of the [O I] 6300 Å forbidden line in HD 122563 is particularly difficult given that its low radial velocity of $v_r = -26.4$ km s^{-1} places this line too close not only to the oxygen sky line at the same (original) wavelength, but also to numerous telluric lines present in this region; only in certain periods of the year does the line appear unblended. This is why so few studies of the forbidden line in this star are available; essentially, the only one presenting the spectrum is that of Lambert, Sneden, & Ries (1974), who measured an equivalent width of EW([O I] 630 nm) = 6.0 ± 1.0

TABLE 7
IR OH LINES: IDENTIFICATION, EQUIVALENT WIDTHS, AND ABUNDANCES

λ (Å)	σ (cm^{-1})	log *gf*	χ (eV)	Branch	*J*″	*v*′, *v*″	EW (mÅ)	[O/Fe]$_1$	[O/Fe]$_2$
15278.52.....	6543.347	−5.382	0.205	P1e	9.5	2, 0	13.	1.05	0.84
15281.05.....	6542.265	−5.382	0.205	P1f	9.5	2, 0	11.0	0.97	0.76
15535.46.....	6435.128	−5.230	0.507	P1e	5.5	3, 1	5.6	0.89	0.71
15536.71.....	6434.613	−5.230	0.507	P1f	5.5	3, 1	5.5	0.88	0.68
15560.24.....	6424.879	−5.307	0.304	P2e	10.5	2, 0	12.0	1.00	0.77
15568.78.....	6421.356	−5.269	0.299	P1e	11.5	2, 0	13.0	1.04	0.84
15572.08.....	6419.994	−5.269	0.300	P1f	11.5	2, 0	12.0	1.02	0.80
15651.90.....	6387.257	−5.132	0.534	P1e	6.5	3, 1	6.3	0.91	0.69
15653.48.....	6386.611	−5.133	0.534	P1f	6.5	3, 1	7.1	0.91	0.74
15897.70.....	6288.500	−5.172	0.412	P1f	13.5	2, 0	11.0	0.98	0.75
15910.42.....	6283.473	−4.976	0.600	P1e	8.5	3, 1	9.0	0.96	0.70
15912.73.....	6282.561	−4.976	0.600	P1f	8.5	3, 1	8.0	0.91	0.68
16190.13.....	6174.915	−4.893	0.688	P2f	9.5	3, 1	11.0	1.03	0.82
16192.13.....	6174.153	−4.893	0.688	P2e	9.5	3, 1	10.0	0.99	0.77
16204.08.....	6169.601	−4.851	0.683	P1e	10.5	3, 1	8.0	0.84	0.60
16255.02.....	6150.266	−5.087	0.538	P1e	15.5	2, 0	7.3	0.91	0.69

NOTE.—[O/Fe]$_1$: $T_{\rm eff} = 4600$ K, $\log g = 1.1$, [Fe/H] = −2.80. [O/Fe]$_2$: $T_{\rm eff} = 4600$ K, $\log g = 1.5$, [Fe/H] = −2.71.

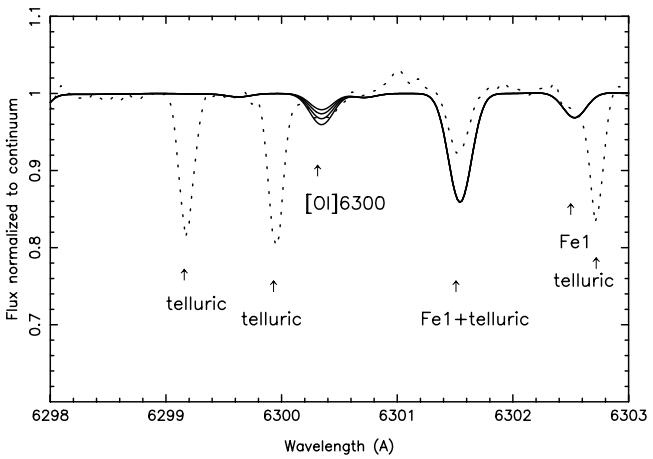

FIG. 5.—[O I] 6300.311 Å line in HD 122563: observed spectrum (*dotted line*) compared to synthetic spectra computed with [O/Fe] = +0.4, +0.5, +0.6, and +0.7 (*solid lines*) for model 2 of Table 5. The value [O/Fe] = +0.6 is adopted. Telluric lines are indicated.

mÅ, whereas Westin et al. (2000) give results based on synthetic spectra.

Our observed spectrum of HD 122563 at the [O I] 6300 Å region is presented in Figure 5. We have measured an equivalent width of EW([O I] 6300 Å) = 6.4 ± 0.5 mÅ. The oscillator strength of the forbidden oxygen line has been recently revised by Allende Prieto, Lambert, & Asplund (2001), because of the presence of a Ni I line, and their study indicates $\log gf = -9.71$, rather than the value of $\log gf = -9.76$ previously given in the literature; we adopt the newer value. This results in [O/Fe] = 0.6 ± 0.1, as shown in Figure 5.

The solar oxygen abundance has also been recently revised by Holweger (2001) and Allende Prieto et al. (2001). The main change in the solar oxygen abundance is due to the presence of a Ni I line not considered before. It is found to be $\epsilon(O) = 8.74$ and 8.69 by Holweger (2001) and Allende Prieto et al. (2001), respectively. Grevesse, Noels, & Sauval (1996) reported $\epsilon(O) = 8.87$, whereas Grevesse & Sauval (1998) give $\epsilon(O) = 8.83$. The value from Allende Prieto et al. (2001) is obtained with three-dimensional model atmospheres, whereas if one-dimensional model atmospheres are used a value of $\epsilon(O) = 8.77$ is obtained. We should adopt the latter value here for consistency, given that we use one-dimensional model atmospheres. However, to be consistent with our previous work (Meléndez et al. 2001; MB02), we adopted the value $\epsilon(O) = 8.87$ (Grevesse et al. 1996); in order to be in agreement with the work of Allende Prieto et al., our results would have to be increased by 0.1 dex.

3.7. *Errors*

The errors due to uncertainties in $T_{\rm eff}$, $\log g$, and v_t were inspected by computing the results for $\Delta T_{\rm eff} = 100$ K, $\Delta \log g = 0.5$ dex, and $\Delta v_t = 0.5$ km s^{-1}. The estimated errors are reported in Table 8.

3.8. *Comparison with the Literature*

Cavallo, Pilachowski, & Rebolo (1997) have derived [O/Fe] = +0.91 ± 0.32 based on the O I triplet lines at 7771.954, 7774.177, and 7775.395 Å. These lines are very faint

TABLE 8

SENSITIVITY TO $T_{\rm EFF}$, LOG g, AND v_t FOR HD 122563

Abundance	$\Delta T_{\rm eff}$ (+100 K)	$\Delta \log g$ (+0.5 dex)	Δv_t (+0.5 km s^{-1})	$(\Sigma x^2)^{1/2}$
[Fe I/H].....	+0.14	−0.11	−0.07	0.19
[Fe II/H].....	−0.03	+0.13	−0.06	0.15
$[O/H]_{OH}$	+0.23	−0.19	+0.03	0.27
$[O/Fe\ I]_{OH}$.....	+0.09	−0.08	+0.10	0.12
$[O/Fe\ II]_{OH}$....	+0.26	−0.32	+0.09	0.42
$[O/H]_{[O\ I]}$.....	+0.08	+0.18	−0.01	0.20
$[O/Fe\ I]_{[O\ I]}$....	−0.06	+0.29	+0.06	0.30
$[O/Fe\ II]_{[O\ I]}$...	+0.11	+0.05	+0.05	0.13
$[O/H]_{O\ I}$	−0.13	+0.23	−0.01	0.26
$[O/Fe\ I]_{O\ I}$.....	−0.27	+0.34	+0.06	0.44
$[O/Fe\ II]_{O\ I}$.....	−0.10	+0.10	+0.05	0.15

in our spectra (Fig. 6); we measured an equivalent width of 2.2 mÅ for the λ7771.954 line, and computed [O/Fe] = +1.1, as given in Table 5, in agreement with Cavallo et al. This result confirms that the O I permitted lines tend to give higher oxygen abundances than the forbidden lines (Spite & Spite 1991; Kiselman 2001, 2002; Lambert 2002).

Lambert et al. (1974) have derived [O/Fe] = +0.6, assuming [Fe/H] = −2.72 and an [O I] line of EW([O I] 6300 Å) = 6.0 ± 1.0 mÅ. Westin et al. (2000) determined stellar parameters of $T_{\rm eff} = 4500$ K, $\log g = 1.3$, [Fe/H] = −2.74, $v_t = 2.5$ km s^{-1}, and derived [O/Fe] = +0.61, adopting $\log gf$([O I] 6300) = −9.75. This result has been obtained by means of synthetic spectra fitting. Both of these results are in very good agreement with the present derivation.

Based on IR OH lines in the *H* band, Balachandran, Carr, & Carney (2001, 2002) obtained [O/Fe] = +0.9 for a giant of [Fe/H] = −3.0 and [O/Fe] = +0.7 for two giants of [Fe/H] = −2.7, one of them being HD 122563 (S. C. Balachandran 2002, private communication); they are thus in agreement with the present results.

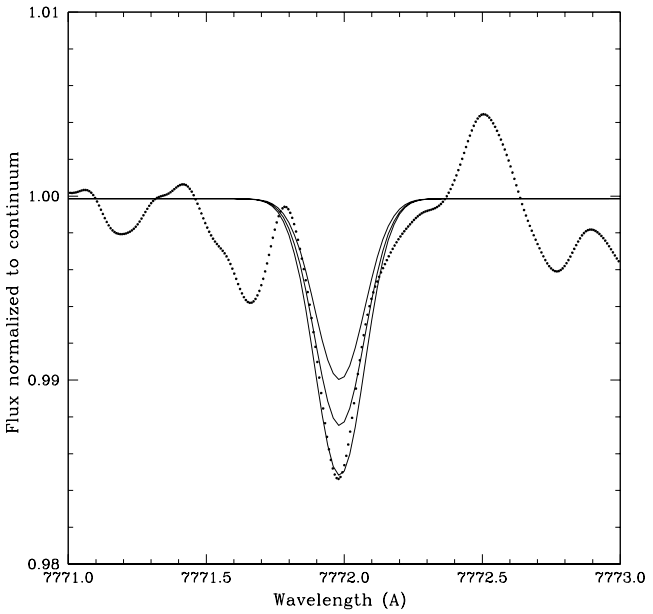

FIG. 6.—O I 7771.9 Å line in HD 122563: observed spectrum (*dotted line*) compared to synthetic spectra computed with [O/Fe] = +0.9, +1.0, and +1.1 (*solid lines*) for model 2 of Table 5.

4. DISCUSSION

HD 122563 is among the best studied metal-poor giants. It has an accurate photometry and a null reddening $E(B-V) = 0.0$, which makes this star a potential template for metal-poor giants. Our oxygen abundance results are summarized in Table 5.

The photometry provides a temperature $T_{\rm eff} = 4600$ K, whereas $T_{\rm eff} = 4450$ K is found from excitation equilibrium of Fe I lines by Johnson (2002). Note, however, that Fe I lines show NLTE effects (Thévenin & Idiart 1999; Dalle Ore 1993), so we prefer to use the photometric temperature. The ionization equilibrium also might not be verified because of NLTE effects on the Fe I lines, and in fact the gravity deduced from the *Hipparcos* parallax is higher than that given by ionization equilibrium.

Nevertheless, the two sets of parameters result in essentially the same oxygen-to-iron ratio, [O/Fe] = 0.6 from the [O I] 6300 Å line and [O/Fe] = 1.1 from the O I 7770 Å line, whereas by using the IR OH lines, model 1 (in which ionization equilibrium is assumed) gives [O/Fe] = 0.84–1.05, but model 2, in which a *Hipparcos* gravity is assumed, gives [O/Fe] = 0.6–0.84. Mean values of [O/Fe] = +0.9 and for model 1 and [O/Fe] = +0.7 for model 2 were adopted. From the oxygen abundance point of view, model 2 is to be preferred, because of a better agreement with the forbidden line. The hydride lines are very sensitive to surface gravities, such that gravities derived from the Fe ionization equilibrium yield an [O/Fe] value higher than that found with the *Hipparcos* parallax.

4.1. *Reliability of* [O I] *and IR* OH *Lines*

The oxygen abundance derived from the forbidden [O I] 6300 Å line is a robust indicator because (1) the lower level of the transition is the ground state of O I, the reservoir of the element oxygen; and (2) NLTE effects have been shown to be negligible for this line and for the other line of the doublet, as stated by Kiselman (2001): "A typical NLTE calculation shows them [the 6300 and 6363 Å [O I] lines] to be exceedingly close to LTE, *both* in line opacity and in line source function."

Another issue is granulation effects (see Fig. 8 of Nissen et al. 2002), which to some extent can be checked using Sc II, which shows lines with $\chi_{\rm ex} = 1.5$ eV instead of 3.0 as for Fe II. Our ratio [O I]/Sc II = 0.49, lower by the amount predicted if the true abundances of Fe and Sc vary in lock step, as suggested by previous work (e.g., Sneden & Primas 2001; Depagne et al. 2002). If this reflects the effect of granulation, then the true ratio [O/Fe] is 0.4 instead of 0.6 (see Figs. 9 and 10 in Nissen et al. 2002). We must wait for an NLTE study of granulation effects in order to see whether this is so, or whether we must keep the [O/Fe] = 0.6 ± 0.15 value.

The IR OH lines at 1.6 μm are also better suited than the UV or 3.2 μm OH lines. This is because there is a minimum of H^- continuum absorption in this spectral region; therefore, the OH lines form deeper and are consequently less affected by temperature fluctuations seen in outer layers of three-dimensional model calculations. On the other hand, it is clear that the two sets of models give distinct results (last column of Table 5), showing that gravity plays a major role in the derivation of oxygen abundances from OH lines.

In Figure 7 we plot [O/Fe] versus [Fe/H] based on IR OH lines (with data points from MB02) and the results for HD 122563 (Table 5, model 2). We favored the oxygen abundances from the lines of lower equivalent widths, recalling that there is a trend of oxygen abundance versus equivalent width.

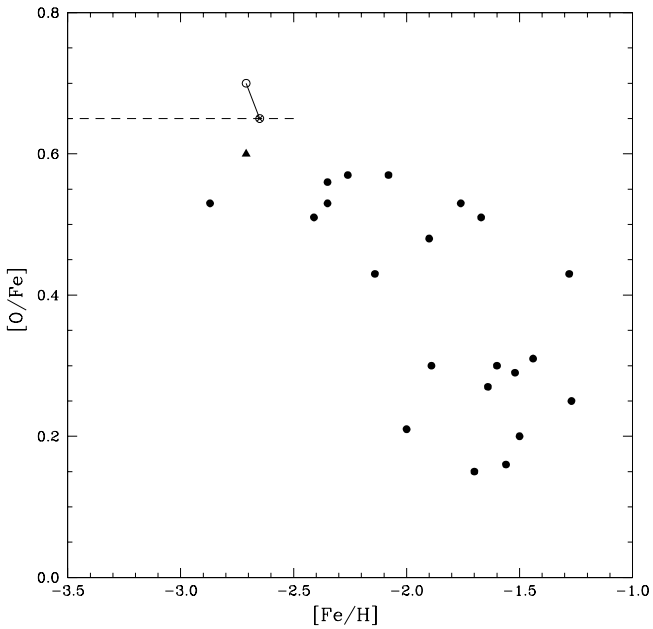

FIG. 7.—[O/Fe] vs. [Fe/H] based on IR OH lines: filled circles correspond to results from MB02; open circle to HD 122563, derived from OH lines in the present work; open circle with a cross is the corrected oxygen abundance from IR OH lines normalized to derivations of MB02 (see § 3.2); filled triangle is the oxygen abundance derived from the forbidden [O I] 6300 Å. All selected results in this figure used model 2 of Table 5. The dashed line corresponds to results by Depagne et al. (2002) of [O/Fe] = +0.65 based on high-S/N [O I] 6300 Å lines in giants of metallicities $-3.5 <$ [Fe/H] < -2.5.

The case of HD 122563 illustrates the problem of oxygen abundance determination in metal-poor stars using one-dimensional model atmospheres. Our discussion should be useful for studies of other, less well known giants.

5. OTHER ELEMENTS

The abundances of other elements in HD 122563 are outside the main scope of this paper. They were nevertheless derived, and the results for some elements (Table 6) deserve to be mentioned: (1) the α-elements Mg, Si, and Ca are overabundant by about [Mg, Si, Ca/Fe] $\approx +0.4$; (2) Ti is not a typical α-element but behaves like one in general; however, in HD 122563 it is less overabundant than the other α-elements; (3) K is also overabundant by about 0.4 dex; (4) Al is deficient, but the blue lines used show strong NLTE effects; (5) Zn is slightly overabundant.

6. CONCLUSIONS

We have shown that the IR OH lines are very useful for O abundance determinations down to very low metallicities and thus provide a major scientific driver for high-resolution infrared spectrographs. We have highlighted the fact that the agreement between different O abundance indicators depends on a suitable choice of atmospheric parameters. On the one hand, with $\log g = 1.5$ the abundance from the IR OH lines is in good agreement with the [O I] 6300 Å line. On the other hand, with $\log g = 1.1$ the O/Fe ratio

derived from the IR OH lines is too large with respect to that derived from the [O I] 6300 Å line. The *Hipparcos* parallax implies $\log g = 1.5$, which we believe to be the best available estimate of the surface gravity of this star, and achieves agreement within errors between the oxygen abundances from the IR OH lines and the [O I] 6300 Å line.

It also becomes clear that, for abundance ratios, by selecting reliable lines (e.g., using the [O I] and Fe II lines to measure the oxygen-to-iron ratios), the systematic errors may be kept small.

What is relevant here is that the surface gravity derived from ionization equilibrium is not satisfactory. Possible causes are the disturbing NLTE effects on Fe I and/or problems with the structure of the one-dimensional models in use. Both will have to be investigated in detail in the future. What is discomforting is that our results cast doubt on O abundances (and those of all other gravity-sensitive elements, for that matter) in all those metal-poor stars for which the ionization equilibrium is the only handle we have on gravity, and these are the vast majority of metal-poor stars. The good news is that in our future lies the *GAIA* satellite, which is expected to measure accurate parallaxes for millions of stars.

Our data, together with those of MB02, seem to support the notion that the [O/Fe] ratio shows both a scatter and a slight increase with decreasing metallicity, as already pointed out in Meléndez et al. (2001) and MB02, in good agreement with predictions of chemical evolution models by Chiappini, Romano, & Matteucci (2003). However, the effects of temperature fluctuations in three-dimensional model atmospheres are stronger in the more metal poor stars, causing a more pronounced decrease of the oxygen abundances derived; Depagne et al. (2002) also find essentially a plateau at $[O/Fe] = +0.65$ based on high S/N [O I] 6300 Å lines in giants of metallicities $-3.5 < [Fe/H] < -2.5$. This evidence contradicts the notion that the oxygen abundances in very metal poor stars should keep increasing with decreasing metallicity.

The roles of second-order effects, such as granulation (Asplund & Garcia Perez 2001; Nissen et al. 2002), are likely to be better ascertained in the next few years by new observations and theoretical computations; meanwhile, it is important to increase the database with high-quality observations. In this respect it would be very important to also observe the OH UV lines of HD 122563, which are formed at a very different depth in the atmosphere. This would allow us to gain insight into its atmospheric structure.

We are grateful to A. M. Magalhães for a revision of the manuscript. We acknowledge partial financial support from FAPESP, CNPq, and the agreement CNPq/CNRS 910068/00-3. J. M. acknowledges FAPESP postdoctoral fellowship 01/01134-3 and CONCYTEC grant 156-2002. C. A. O. Torres acknowledges CNPq grant 200256/02.0. The FEROS observations at the European Southern Observatory (ESO) were carried out within the Observatório Nacional ON/ESO and ON/IAG agreements, under Fapesp project 1998/10138-8. The infrared observations were obtained by staff members of the Gemini Observatory, which is operated by the Association of Universities for Research in Astronomy, Inc., under a cooperative agreement with the NSF on behalf of the Gemini partnership: US, UK, Canada, Chile, Australia, Brazil, and Argentina. The infrared data presented here were obtained at the W. M. Keck Observatory, which is operated as a scientific partnership among the California Institute of Technology, the University of California, and NASA. The Observatory was made possible by the generous financial support of the W. M. Keck Foundation. The Very Large Telescope (VLT) is operated by the European Southern Observatory. We have made use of data from the *Hipparcos* astrometric mission of the ESA.

REFERENCES

Abrams, M. C., Davis, S. P., Rao, M. L. P., Engleman, R., Jr., & Brault, J. W. 1994, ApJS, 93, 351
Allende Prieto, C., Lambert, D. L., & Asplund, M. 2001, ApJ, 556, L63
Alonso, A., Arribas, S., & Martínez-Roger, C. 1998, A&AS, 131, 209
———. 1999a, A&AS, 140, 261 (AAM99a)
———. 1999b, A&AS, 139, 335 (AAM99b)
Alvarez, R., & Plez, B. 1998, A&A, 330, 1109
Anstee, S. D., & O'Mara, B. J. 1995, MNRAS, 276, 859
Anstee, S. D., O'Mara, B. J., & Ross, J. E. 1997, MNRAS, 284, 202
Asplund, M., & García-Pérez, A. E. 2001, A&A, 372, 601
Asplund, M., Gustafsson, B., Kiselman, D., & Eriksson, K. 1997, A&A, 318, 521
Balachandran, S. C., Carr, J. S., & Carney, B. W. 2001, NewA Rev., 45, 529
———. 2002, Highlights Astron., 12, 420
Barklem, P. S., & O'Mara, B. J. 1997, MNRAS, 290, 102
Barklem, P. S., O'Mara, B. J., & Ross, J. E. 1998, MNRAS, 296, 1057
Bell, R. A., Eriksson, K., Gustafsson, B., & Nordlund, A. 1976, A&AS, 23, 37
Biémont, E., Baudoux, M., Kurucz, R. L., Ansbacher, W., & Pinnington, A. E. 1991, A&A, 249, 539
Boesgaard, A. M., King, J. R., Deliyannis, C. P., & Vogt, S. S. 1999, AJ, 117, 492
Carretta, E., Gratton, R. G., & Sneden, C. 2000, A&A, 356, 238
Castilho, B. V., Spite, F., Barbuy, B., Spite, M., De Medeiros, J. R., & Gregorio-Hetem, J. 1999, A&A, 345, 249
Cavallo, R. M., Pilachowski, C. A., & Rebolo, R. 1997, PASP, 109, 226
Cayrel, R., Perrin, M.-N., Barbuy, B., & Buser, R. 1991, A&A, 247, 108
Cayrel, R., & Steffen, M. 2000, in IAU Symp. 198, The Light Elements and Their Evolution, ed. L. da Silva, M. Spite, & J. R. de Medeiros (San Francisco: ASP), 437
Chen, B.,Vergely, J. L., Valette, B., & Carraro, G. 1998, A&A, 336, 137
Chiappini, C., Romano, D., & Matteucci, F. 2003, MNRAS, 339, 63
Coxon, J. A., & Foster, S. C. 1992, Canadian J. Phys., 60, 41
Dalle Ore, C. 1993, Ph.D. thesis (Lick Observatory, Univ. California, Santa Cruz)
Depagne, E., et al. 2002, A&A, 390, 187
Edvardsson, B., Andersen, J., Gustafsson, B., Lambert, D. L., Nissen, P. E., & Tomkin, J. 1993, A&A, 275, 101
Goldman, A., Shoenfeld, W. G., Goorvitch, D., Chackerian C., Jr., Dothe, H., Mélen, F., Abrams, M. C., & Selby, J. E. A. 1998, J. Quant. Spectrosc. Radiat. Transfer, 59, 45
Grevesse, N., Noels, A., & Sauval, J. 1996, in ASP Conf. Ser. 99, Cosmic Abundances, ed. S .S. Holt & G. Sonneborn (San Francisco: ASP), 117
Grevesse, N., & Sauval, A. J. 1998, Space Sci. Rev., 85, 161
Gustafsson, B., Bell, R. A., Eriksson, K., & Nordlund, Å. 1975, A&A, 42, 407
Hakkila, J., Myers, J. M., Stidham, B., & Hartmann, D. H. 1997, AJ, 114, 2043
Hauck, B., & Mermilliod, M. 1998, A&AS, 129, 431
Hill, V., et al. 2002, A&A, 387, 560
Holweger, H. 2001, in AIP Conf. Proc. 598, Solar and Galactic Composition, ed. R.F. Wimmer-Schweingruber (Melville: AIP), 23
Huber, K. P., & Herzberg, G. 1979, Constants of Diatomic Molecules (New York: Van Nostrand Reinhold)
Israelian, G., García López, R., & Rebolo, R. 1998, ApJ, 507, 805
Israelian, G., Rebolo, R., García López, R., Bonifacio, P., Molaro, P., Basri, G., & Shchukina, N. 2001, ApJ, 551, 833
Johnson, J. 2002, ApJS, 139, 219
Kaufer, A., et al. 2000, Proc. SPIE, 4008, 459
Kiselman, D. 1998, A&A, 333, 732
———. 2001, NewA Rev., 45, 559
———. 2002, Highlights Astron., 12, 429
Kraft, R. P., Suntzeff, N. B., Langer, G. E., Carbon, D. F., Trefzger, C. F., Friel, E., & Stone, R. P. S. 1982, PASP, 94, 55
Kupka, F. G., Ryabchikova, T. A., Piskunov, N. E., Stemples, H. C., & Weiss, W. 2000, Baltic Astron., 9, 590
Lambert, D. L. 2002, Highlights Astron., 12, 445

Lambert, D. L., Sneden, C., & Ries, R. M. 1974, ApJ, 188, 97
McLean, I. S., et al. 1998, Proc. SPIE, 3354, 566
Meléndez, J. 1999, MNRAS, 307, 197
Meléndez, J., & Barbuy, B. 1999, ApJS, 124, 527
———. 2002, ApJ, 575, 474 (MB02)
Meléndez, J., Barbuy, B., & Spite, F. 2001, ApJ, 556, 858
Nissen, P. E., Høg, E., & Schuster, W. 1997, in *Hipparcos* Venice '97 (ESO SP-402; Garching: ESO), 225
Nissen, P., Primas, F., Asplund, M., & Lambert, D. L. 2002, A&A, 390, 235
O'Brian, T. R., et al. 1991, J. Opt. Soc. Am. B, 8, 1185
Perryman, M. A. C., et al. 1997, A&A, 323, L49
Plez, B., Brett, J. M., & Nordlund, Å. 1992, A&A, 256, 551
Plez, B., Smith, V. V., & Lambert, D. L. 1993, ApJ, 418, 812
Sneden, C. 1973, ApJ, 184, 839
Sneden, C., & Primas, F. 2001, NewA Rev., 45, 513
Spite, M., & Spite, F. 1991, A&A, 252, 689
Stone, R. P. S. 1983, PASP, 95, 27
Thévenin, F., & Idiart, T. 1999, ApJ, 521, 753
Wallerstein, G., Greenstein, J. L., Parker, R., Helfer, H. L., & Aller, L. H. 1963, ApJ, 137, 280
Westin, J., Sneden, C., Gustafsson, B., & Cowan, J. J. 2000, ApJ, 530, 783